The high-concentration stable phase: The breakthrough of catanionic surfactant aqueous system

Shasha Jiang [a,b], Weilin Qi [a], Cheng Ma [a], Tongyue Wu [a], Xiaoyu Li [a], Xingyue Chen [c], Shuitao Gao [a], Jinwan Qi [a], Yun Yan [a], Jianbin Huang [a,*]

[a] *College of Chemistry and Molecular Engineering, Peking University, Beijing 100871, China*
[b] *School of Earth & Space Science, Peking University, Beijing 100871, China*
[c] *College of Science, China Agricultural University, Beijing 100193, China*

GRAPHICAL ABSTRACT
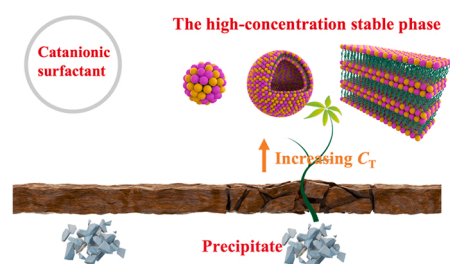
ARTICLE INFO

ABSTRACT

Precipitates occur readily in the aqueous mixture of cationic and anionic surfactants. We report that the precipitates formed in the catanionic surfactant systems at charge ratios deviated from 1:1 can be solubilized by simply increasing the total surfactant concentrations. At higher concentrations, there are vesicles in the supernatant, which will sequester the monomer surfactant in equilibrium with the precipitates. This shifts precipitation-solvation equilibrium continuously. As a result, the precipitates vanish when all the surfactants in the precipitates are taken into the vesicles. In this way, a high-concentration stable phase (HCSP) can be formed in the precipitated surfactant systems, which can be generalized to all catanionic surfactant systems. We envision the concentration-triggered HCSP is very promising in guiding the large-scale application of catanionic surfactants.

1. Introduction

Surfactants have been widely utilized in the field of industrial manufacturing [1,2], agricultural production [3–6] and basic scientific research [7,8], stemming from their excellent interface activity and rich aggregation behaviors. It has long been recognized that well organized assemblies rather than free molecules endow the surfactant solutions with excellent performance [9–13]. The ideal concentration of surfactant systems with desired functions is usually at least 3–5 times of their CMC (the critical micelle concentration). For this reason, considerable

efforts were endeavored to develop functional surfactant systems with low CMC [14–22], both in terms of research value and economic benefits.

Catanionic surfactant (i.e. mixtures of cationic and anionic surfactants) is one of the desired systems with extremely low CMC, which is one or two orders of magnitude lower than single ionic surfactants [16, 20–22]. Since E. W. Kaler's discovery of vesicles in the aqueous systems of catanionic surfactants in 1989 [23], considerable efforts have been endeavored to study the self-assembling behavior of catanionic surfactants [16,20–22,24–29]. Considering the fact that there are amazingly rich hydrophobic domains in these surfactant self-assembled structures, it seems very promising to utilize the catanionic surfactants in diversified industries, such as oil recovery [30–32], environmental management [28] and pharmacy [29]. However, the problems of easy precipitation and phase separation in most catanionic systems have greatly restricted their practical applications.

Theoretically, monovalent anionic and monovalent cationic surfactant preferentially form 1:1 ion pairs in aqueous solution due to the strong electrostatic attraction and the synergistic hydrophobic effect [33]. This tendency is so predominant that the composition of the surface adsorption layer in a catanionic surfactant system is always near 1:1 regardless of the real molar ratio of the entire system [34]. In solution, these ion-pairs would aggregate to form large microstructures which finally lead to precipitates or phase separation [26, 35–37]. In order to improve the fraction of catanionic surfactants in solution, which is in the form of micelles or vesicles, many researchers focused on improving its solubility by modifying the surfactant structure with more hydrophilic head group or addition of organic additives such as propanol [14,15,38, 39]. However, these strategies will considerably increase the CMC, which inevitably decreases the efficiency of the catanionic surfactants since the monomers would not contribute to the desired functions. It is therefore of significant importance to endow the catanionic surfactant systems with low CMC but high solution concentration, namely, with high ratio of solution concentration to CMC.

It is noticed that the CMC for the catanionic surfactant systems is not sensitive to the mixing ratio [34]. Because the CMC for the mixed system is usually one or two orders lower than each of the single system [16, 20–22], variation of the mixing ratio would not change the order of the CMC [34]. This inspires that we may obtain stable catanionic surfactant systems with high total concentrations by controlling the mixing ratio. However, so far, study in this regard is far less than enough.

Herein we report the high-concentration stable phase formation in the catanionic surfactant systems which is facilitated by enhanced concentration. We show that in most catanionic surfactant systems, precipitates may form at low concentrations regardless of the mixing ratio. However, the precipitates in systems with molar ratios deviated from 1:1 will vanish again simply by increasing concentration. This phenomenon is universal for a large variety of catanionic surfactant systems, indicating the nirvana rebirth of catanionic surfactant systems.

2. Experimental section

2.1. Materials

Dodecylpyridinium chloride (DPyCl, 99%), Octyltrimethylammonium chloride (OTAC, 99%), Decyltrimethylammonium chloride (DeTAC, 99%) and Dodecyl lauric acid (SL, 99%) were purchased from Aladdin. Sodium dodecyl sulfate (SDS, 98%), Sodium octyl sulfonate ($SOSO_3$, 99%) and Sodium octyl sulfate ($SOSO_4$, 98%) were purchased from Macklin. Dodecyltrimethylammonium chloride (DTAC, 99%) was purchased from Energy chemical. Dodecyl triethyl ammonium bromide (DTEAB) was made in laboratory. 1-Dodecyl-3-methylimidazolium chloride (DMImC, 99%) was purchased from 3 A Materials. Benzyldimethyldodecylammonium chloride (BDDAC, 99%) and Decyl sodium sulfate (SDeS, 98%) were purchased from TCI. All reagents were used without other purification. Milli-Q water of 18 MΩ is used to prepare aqueous solutions.

2.2. Sample preparation

Calculated amounts of surfactant were weighed to prepare stock solution in volumetric flask. Samples were obtained by mixing the stock solutions of anionic and cationic surfactants at a desired mixing ratio and concentration. The investigated C_T (total concentration) of DPyCl and SDS covered a broad range from 0 to 2000 mM. After sealing, Samples were vortically mixed and then equilibrated in a temperature incubator controlled to 25 °C for 24 h before observation and other experiments.

2.3. Negative-staining transmission electron microscopy (NS-TEM)

NS-TEM images were obtained by using Tecnai T20 operated at an accelerating voltage of 200 kV. A drop of the sample (~10 µL) was added onto a carbon-coated copper grid (300 mesh) and was stained with 3% uranyl acetate to retain 3 min. The excess sample and staining agent were wiped away with filter paper. The specimens were kept in air overnight before observation.

2.4. Freeze-fracture transmission electron microscopy (FF-TEM)

Freeze fracture and replication technique were carried out to get microstructures of surfactant solutions. Before carried out in a high-vacuum freeze-fracture apparatus (Balzers BAF 400D), a specimen holder with a drop of the solution was cooled by plunging into liquid nitrogen. The replicas composed of carbon were shifted onto copper grids and measured on Tecnai T20 (200 kV).

2.5. Rheology

The rheological properties of the samples about 10 mL were measured at 25 °C with a Thermo Hake RS300 rheometer.

2.6. Elemental Analysis

The elemental analyses were carried out on a Vario EL elemental analyzer (Elementar Analysensysteme GmbH, Langenselbold, Germany).

2.7. Ultraviolet-visible spectrophotometer

UV–vis absorbance measurements were carried out on a UV-1800 SHIMADZU spectrophotometer (Hitachi. Ltd., Tokyo, Japan), and 1 cm quartz cuvets were used. All spectral measurements were recorded at 25 ℃.

The standard curve of DPyCl was measured at maximum absorbing wavelength of 259 nm.

2.8. Dynamic light scattering (DLS)

DLS data were obtained by a BI-200 SM instrument. The samples were filtered by 800 nm filters to avoid dust before measurements. Measurements were made at the scattering angle of 90º and the analysis method used was CONTIN. All measurements were conducted using deionized water at 25 °C.

2.9. Surface tension

Surface tension (γ) measurements were performed on a surface tensiometer (Dataphysics DCAT21) using the Wilhelmy plate method at 25.0 ± 0.5 °C by a thermostatic bath used to dominate the temperature of the measurement cell. Each sample was equilibrated for about 30 min, and each experiment was performed in triplicate.

3. Results and discussion

3.1. The high-concentration stable phase in mixed DPyCl/SDS system

Fig. 1**a** shows the phase diagram of DPyCl/SDS system and the corresponding three types of phase behaviors, in which precipitation covers a broad range of C_T and x_{DPyCl}. However, at stoichiometries deviated from the electroneutral mixing ($0.01 < x_{DPyCl} \leq 0.33$, $0.83 \leq x_{DPyCl} < 0.99$), the precipitates are formed at low surfactant concentrations but they vanish with increasing concentration. Here, this reoccurred stable phase is defined as high-concentration stable phase (HCSP), which could keep stable for more than one year.

To understand what occurs in the transition from precipitates to HCSP, the system of $x_{DPyCl} = 0.25$ is taken for further analysis. According to phase behaviors, the regions I to IV are designated with increasing concentration (Fig. 1b). Region I is clear solution where no micelles are formed as examined by TEM and DLS (Fig. S1). As C_T increases from 0.08 mM to 6 mM, the system enters into Region II, where precipitates occur (Fig. 1b, II). SEM observation reveals that the precipitates are composed of squares, rectangles, or hexagons (Fig. 2a), whereas monomers or vesicles are formed in the suspension. At concentration lower than 3 mM, only monomers exist (Fig. S2). Vesicles are observed in the concentration range of 3–6 mM. At the concentration of 3 mM, the diameter of large vesicles is about 100 nm (Fig. 2a), whereas it increases to over 1000 nm at 6 mM (Fig. 2b). In line with this, the turbidity in the upper phase increases (Fig. S3).

However, further increase of C_T results in the transformation from precipitates to HCSP. As shown in region III, the samples are stable in a wide C_T range of 6 mM~2000 mM (Fig. 1b, III). According to the TEM and DLS analysis, the microstructures therein are dispersed vesicles, cylindrical micelles, adhesive vesicles, and lamellar structures, with increasing concentration. On the meanwhile, the relative viscosity and

the turbidity change as well (Fig. 1c and Fig. 1d). In the C_T range of 6 mM ~ 15 mM, the samples are water-like and opalescent. Multilayer-vesicles with diameters around 500 nm are observed (Fig. 2c). In this region, the turbidity of the solutions decreases with increasing C_T until the solution becomes transparent at 15 mM. The relative viscosity keeps increasing as the concentration increases from 6 mM to 15 mM, and the steady rheology measurements clearly reveal the non-Newtonian nature for these systems. As shown in Fig. S4, shear-thickening and shear-thinning behaviors take place successively with the increase of shear rate, suggesting the existence of asymmetrical aggregates. The apparent diameters of the aggregates in this system are 15 nm and 50 nm, as evidenced by two scattering peaks (Fig. 2d). Combined with the TEM and DLS results (Fig. 2d), it is found that vesicles coexist with cylindrical micelles in the system. There is no obvious change of sample appearance or aggregated structures until the C_T is up to 100 mM. In the C_T range of 100 mM ~ 500 mM, the turbidity of the solutions increases again. TEM observation reveals that the self-assembled structures have transformed into adhesive vesicles (Fig. 2e), which results in the high relative viscosity. As the C_T increases further over 500 mM, birefringence occurs (Fig. 1d), and lamellar structures are formed (Fig. 2f). Two sets of lamellae are revealed by the XRD measurements, with the interlayer spacings being 37.1 and 33.5 Å, respectively. It is noticed that the diffraction intensity resulted from the spacings of 33.5 Å is much stronger than that of the 37.1 Å analogues, indicating these are the dominant structures. Considering the length of the extended DPyCl and SDS molecule is 19 and 18 Å, respectively, these spacings indicate that the alkyl chain of DPyCl and SDS is interlaced in the bilayers (Fig. S5). Above all, the aggregation behaviors of the DPyCl/SDS system ($x_{DPyCl}=0.25$) in II and III along with C_T are summarized in Fig. 2g. It is worth noting that the aggregate morphologies dependent on C_T in HCSP are relatively different from those in the catanionic surfactant mixtures where the counterions are removed, and the assemblies of these
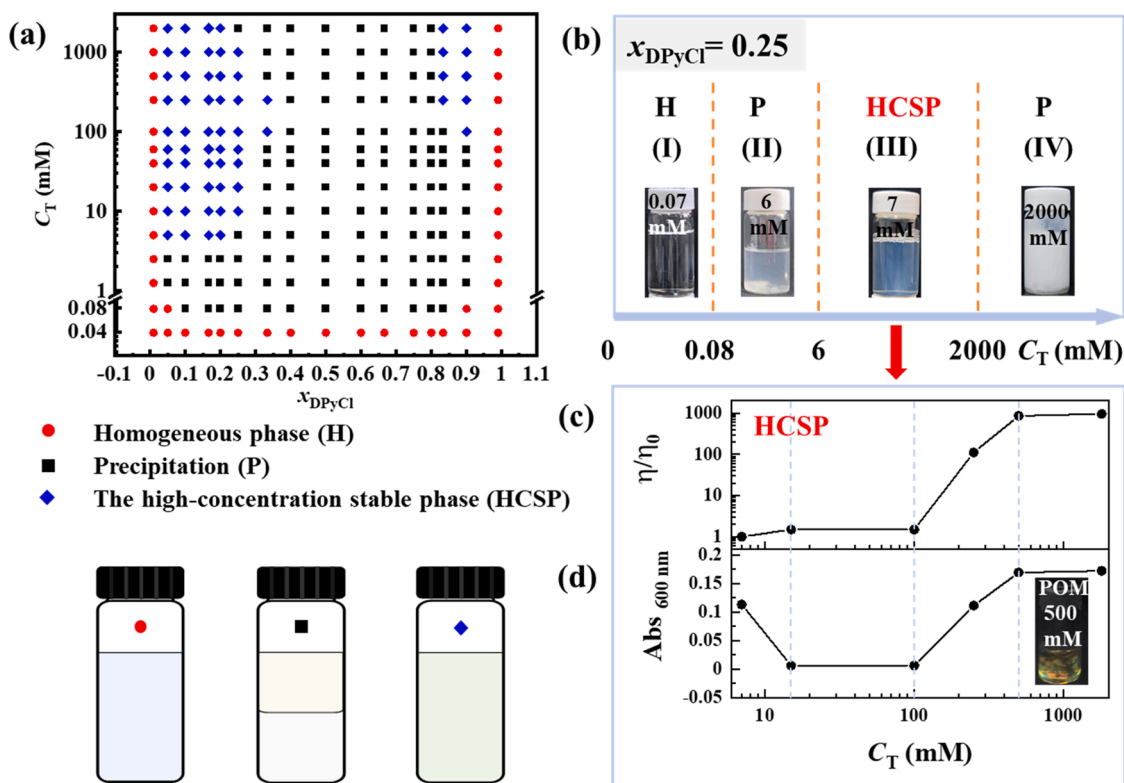

Fig. 1. (a) The phase diagram of DPyCl/SDS system and schematic illustration of the three types of phase behavior: homogeneous phase (H); precipitation (P) and high-concentration stable phase (HCSP). (b) The regions I to IV are assigned from left to right along the C_T axis ($x_{DPyCl}=0.25$. Insets are the macrophotographs: from left to right, $C_T = 0.07$, 6, 7, 2000 mM, respectively. (c) Absorbance and (d) relative viscosity for SPH in Fig. 1b and dashed lines mark the turn. The insert photograph in Fig. 1d is under the polarizer ($C_T =500$ mM).
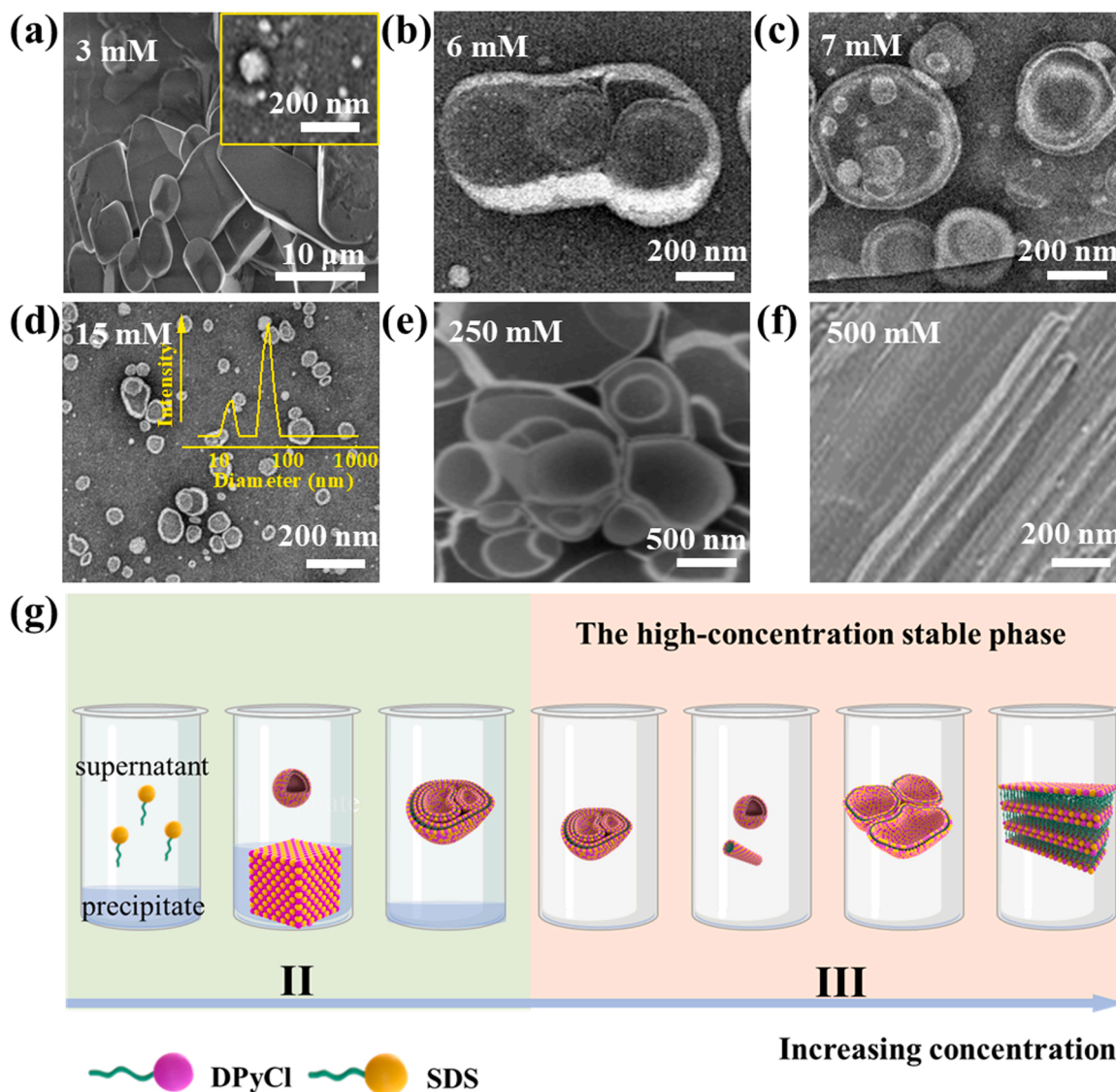
Fig. 2. DPyCl/SDS (x_{DPyCl}=0.25, 25 ℃) systems with varied total surfactant concentrations C_T. (a) $C_T = 3$ mM, SEM image for precipitate and TEM image (inset) for supernatant. (b) $C_T = 6$ mM, TEM image for supernatant. TEM photographs for (c) $C_T = 7$ mM, (d) $C_T = 15$ mM, (e) $C_T = 250$ mM. The inset in Fig. 2e is the DLS result of solution. (f) $C_T = 500$ mM, FF-TEM image. (g) Schematical illustration of the microstructures.

mixtures are unilamellar vesicles independent from the surfactant concentration employed, possibly owing to electroneutral mixing of cationic and anionic surfactants[40–42].

3.2. The mechanism of "high-concentration stable phase"

The formation of HCSP with increasing concentration in the catanionic surfactant systems is closely related to the self-assembly behavior. It is noticed that at C_T lower than 3 mM, no micelles or vesicles are observed in the supernatant. This means that in this low concentration range, there are only electrostatic interactions between the surfactant molecules, and neither of them is able to form single micelles/vesicles nor mixed micelles/vesicles. However, above a critical value, the non-stoichiometric DPyCl and SDS are able to form self-assemble structures. We then expect that the HCSP is a result of shifting of the equilibrium of the precipitation by sequestering the dissolved surfactant molecules from the precipitates into the mixed self-assemblies. Because of the formation of precipitates requires 1:1 mixed surfactant whereas the total molar ratio between DPyCl and SDS is 1:3 in the entire system, the fraction of DPyCl in the upper phase should be very small when the precipitates are initially formed. Therefore, SDS will be enriched in the

upper phase. As a result, the initially formed self-assemblies in the upper phase are negatively charged. These negatively charged self-assemblies are then able to sequester the positively charged DPyCl that enters the upper phase due to the precipitation-solvation equilibrium. This on the one hand will decrease the surface charges of the self-assemblies in the upper phase, leading to the growth of their size, and on the other hand, also results in the solubilization of the precipitates. Indeed, the zeta potential for the vesicles in the 3 mM system is − 43 mV, whereas it becomes − 14 mV as the concentration increases to 6 mM.

To further confirm the above postulation, we conducted Elemental Analysis and Ultraviolet-visible Spectrophotometry to examine the compositions in precipitate and supernatant respectively. The ordinate in Fig. 3a represents the amount of each surfactant (mmol) in the precipitates, namely, n^P, which form in one liter of solution. It is found that the precipitates reach a maximum at $C_T = 4$ mM, then sharply reduce at $C_T = 5$ mM and almost vanish completely at $C_T = 6$ mM. In addition, the precipitation slows at $C_T > 3$ mM, as evidenced by the slope of the $n^P \sim C_T$ curve. Nitrogen and sulphur are characteristic elements for DPyCl and SDS respectively, which can be determined by Elemental Analysis to evaluate the compositions of DPyCl and SDS in precipitate. The molar ratio of SDS:DPyCl in the precipitates (region II, x_{DPyCl}=0.25) is
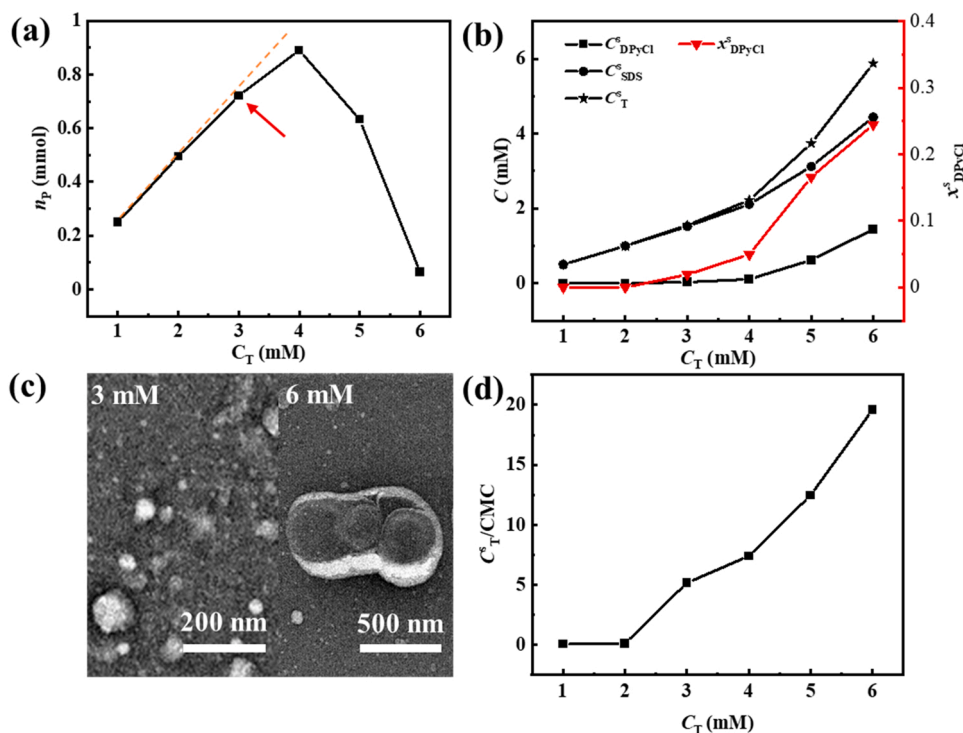
Fig. 3. DPyCl/SDS (x_{DPyCl}=0.25, 25 ℃) systems with varied total surfactant concentrations C_T. (a) Variation of the n^P at different C_T. (b) C^s_{DPyCl}, C^s_{SDS}, C^s_T and x^s_{DPyCl} versus C_T. (c) NS-TEM images for supernatant at $C_T = 3$ mM (left) and $C_T = 6$ mM (right). (d) The ratio of C^s_T/CMC is plotted against C_T.

approximately 1:1 (Table 1) at C_T ranging from 0.08 to 6 mM, with the variations of the concentration of DPyCl, SDS, the total surfactant, and the molar fraction of DPyCl in supernatant, namely, C^s_{DPyCl}, C^s_{SDS}, C^s_T and x^s_{DPyCl}, shown in Fig. 3b. C^s_{DPyCl} is determined by the UV-Vis spectrophotometer method, and thus the amount of DPyCl in precipitate can be speculated by the difference value between the known C^s_{DPyCl} and the total concentration of DPyCl. Additionally, C^s_{SDS} is inferred by the difference value between the known total concentration of SDS and the amount of SDS in precipitate, which is equal to that of DPyCl in precipitate. It is noticed that the cationic surfactant DPyCl is not detected in the supernatant at $C_T < 3$ mM. It starts to appear in the supernatant at $C_T = 3$ mM. Above this concentration, x^s_{DPyCl} increases gradually from 0.02 to 0.24. With the variation of the components in the upper phase, the vesicles grow from 100 nm to 1000 nm (Fig. 3c). This means that the vanishing of the precipitates with increasing concentration is indeed caused by sequestering the DPyCl molecules released from the precipitates due to the precipitation-solvation equilibrium. As a requirement of the charge neutrality in the precipitates, equal amount of SDS should also leave the precipitates and enter the mixed self-assemblies in the upper phase, which finally leads to the complete solubilization of the precipitates. Since the CMC for the DPyCl/SDS at $x_{DPyCl} = 0.25$ remains 0.3 mM, monotonous increase of the ratio of C^s_T/CMC can be expected with increasing concentration (Fig. 3d). This means that we are able to realize low CMC but high solution concentration in catanionic surfactant systems.

Table 1
The ratio of SDS to DPyCl in precipitation at different concentrations.
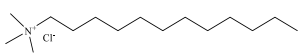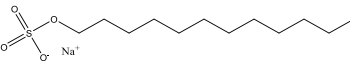
C_T (mM)	SDS/DPyCl
0.08	1/1.00
1	1/0.93
3	1/1.02
6	1/1.02
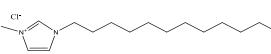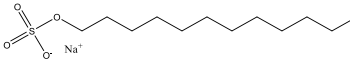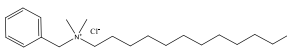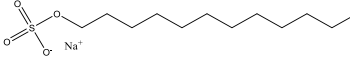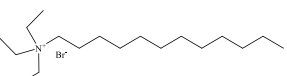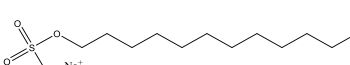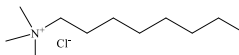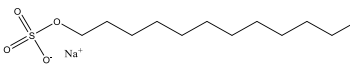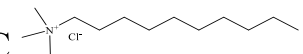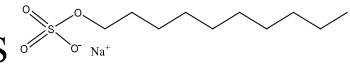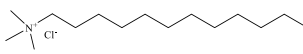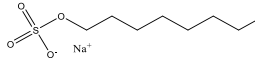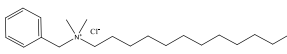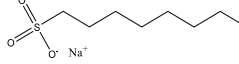
3.3. The universality of high-concentration stable phase

The concentration-triggered HCSP is a universal phenomenon in catanionic surfactant systems. As the surfactant systems varied from the studied SDS-rich SDS/DPyCl system to the DPyCl-rich SDS/DPyCl system, similar HCSP phenomenon was observed (Fig. S6). Furthermore, the concentration-induced HCSP is generally identified for a board range of mixed nonstoichiometrical catanionic surfactant systems (Table 2), where the cationic surfactant heads cover -N⁺(CH₃), -N⁺(C₂H₅), -(NC₆H₅)⁺, and -(CH₃N₂C₃H₃)⁺, and the anionic surfactant heads include -SO₄⁻, -SO₃⁻ and -COO⁻. Abundant microstructures such as micelles, vesicles and lamellar structures are discovered in high-concentration stable phase. For instance, DLS measurement (Fig. 4a) for the DTAC/SDS system ($C_T = 100$ mM, x_{DTAC}=0.2) reveals the presence of particles with average hydrodynamic diameter of 7 nm. TEM examination rules out the possibility of vesicles, indicating they are micelles (Fig. S7). In contrast, lamellae (Fig. 4b) are found in the BDDAC/SOSO₃ system ($C_T = 100$ mM, x_{BDDAC}=0.25), and vesicles are obser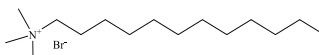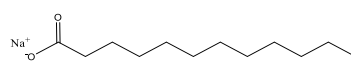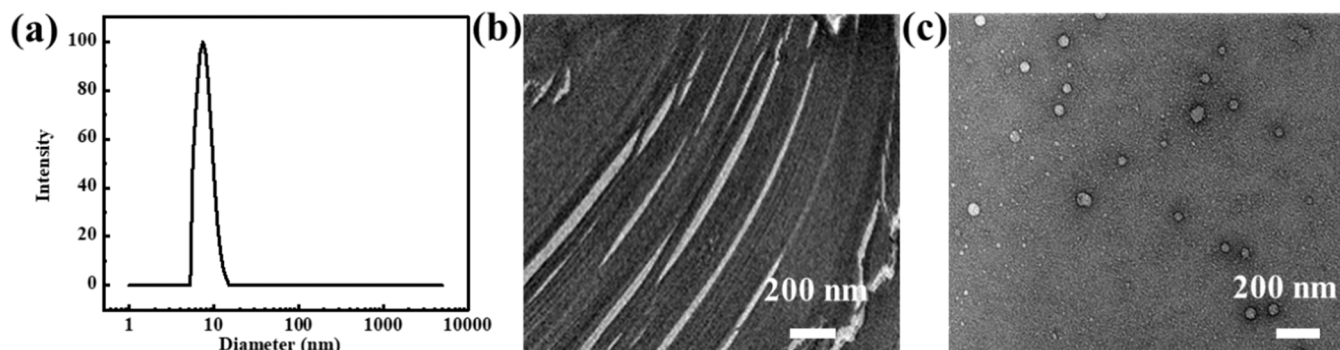ved in the DeTAC/SDeS solution ($C_T = 100$ mM, x_{DeTAC}=0.32) (Fig. 4c). Taken together, these results suggest that the high-concentration stable phase is a universal phenomenon for the entire class of mixed cationic/anionic surfactant systems. In comparison with low-concentration homogeneous phase with monomers inside, the high-concentration stable phase shows promising potential in drug delivery, pesticide encapsulation and other applications, resulting from the abundant self-assembled structures with rich hydrophobic domains.

4. Conclusion

In conclusion, we report that the precipitates formed in the catanionic surfactant systems at charge ratios deviated from 1:1 can be solubilized again by simply increasing the total concentration of the surfactants. The rationale is that at low concentrations the mixed surfactant system tends to form precipitates due to the electrostatic interactions between the oppositely charged surfactant monomers. With increasing concentration, vesicles start to form in the supernatant,

Table 2
Mixtures of anionic and cationic surfactants.

Cationic surfactants	Anionic surfactants	HCSP
DTAC	SDS	🙂
DMImC	SDS	🙂
BDDAC	SDS	🙂
DTEAB	SDS	🙂
OTAC	SDS	🙂
DeTAC	SDeS	🙂
DTAC	SOSO$_4$	🙂
BDDAC	SOSO$_3$	🙂
DTAB	SL	🙂

Fig. 4. (a) DLS measurement for DTAC/SDS system (C_T = 100 mM, x_{DTAC}=0.2). (b) FF-TEM image for BDDAC/SOSO$_3$ system (C_T = 100 mM, x_{BDDAC}=0.25). (c) NS-TEM photograph for DeTAC/SDeS (C_T = 100 mM, x_{DeTAC} =0.32). All experiments were carried at 25 ℃.

which will sequester the monomer surfactants in equilibrium with the precipitates. In this way, all the surfactant molecules in the precipitates will enter the vesicles in the supernatants. This phenomenon is universal for all the tested surfactant systems indicating the precipitated surfactant systems can rebirth. We expect the current study may be very helpful in guiding large-scale application of the mixed systems of cationic and anionic surfactants.

CRediT authorship contribution statement

Shasha Jiang: Conducted most of the experiments and wrote original draft. **Weilin Qi, Cheng Ma, Xiaoyu Li, Shuitao Gao and Jinwan Qi:** Analyzed the data and discussed the results. **Tongyue Wu:** Performed the FF-TEM measurements. **Xingyue Chen:** Provided CMC value. **Yun Yan:** Analyzed the data and revised the paper. **Jianbin Huang:** Designed the study, analyzed the data and discussed the results.

Declaration of Competing Interest

The authors declare that they have no known competing financial interests or personal relationships that could have appeared to influence the work reported in this paper.

Acknowledgement

Appendix A. Supporting information

Supplementary data associated with this article can be found in the online version at doi:10.1016/j.colsurfa.2022.129120.

References

[1] Q.H. Liang, X.J. Liu, G.M. Zeng, Z.F. Liu, L. Tang, B.B. Shao, Z.T. Zeng, W. Zhang, Y. Liu, M. Cheng, Surfactant-assisted synthesis of photocatalysts: mechanism, synthesis, recent advances and environmental application, Chem. Eng. J. 372 (2019) 429–451.

[2] Z.G. Wang, H.T. Zhao, Y. Zhang, A. Natalia, C.A.J. Ong, M.C.C. Teo, J.B.Y. So, H. L. Shao, Surfactant-guided spatial assembly of nano-architectures for molecular profiling of extracellular vesicles, Nat. Commun. 12 (2021) 1–12.

[3] B. Liu, Y.X. Fan, H.F. Li, W.W. Zhao, S.Q. Luo, H. Wang, B. Guan, Q.L. Li, J.L. Yue, Z.C. Dong, Control the entire journey of pesticide application on superhydrophobic plant surface by dynamic covalent trimeric surfactant coacervation, Adv. Funct. Mater. 31 (2021), 2006606-2006606.

[4] M.R. Song, D. Hu, X.F. Zheng, L.X. Wang, Z.L. Yu, W.K. An, R.S. Na, C.X. Li, N. Li, Z.H. Lu, Enhancing droplet deposition on wired and curved superhydrophobic leaves, ACS Nano 13 (2019) 7966–7974.

[5] L.F. He, S.W. Xi, L. Ding, B.X. Li, W. Mu, P.Q. Li, F. Liu, Regulating the entire journey of pesticide application on surfaces of hydrophobic leaves modified by pathogens at different growth stages, ACS Nano (2021).

[6] M. Damak, S.R. Mahmoudi, M.N. Hyder, K.K. Varanasi, Enhancing droplet deposition through in-situ precipitation, Nat. Commun. 7 (2016) 1–9.

[7] M. Barai, M.K. Mandal, A. Karak, R. Bordes, A. Patra, S. Dalai, A.K. Panda, Interfacial and aggregation behavior of dicarboxylic amino acid-based surfactants in combination with a cationic surfactant, Langmuir 35 (2019) 15306–15314.

[8] Z. Zhai, X. Yan, J. Xu, Z. Song, S. Shang, X. Rao, Phase behavior and aggregation in a catanionic system dominated by an anionic surfactant containing a large rigid group, Chem. Eur. J. 24 (2018) 9033–9040.

[9] G.X. Zhao, X.G. Li, Solubilization of n-octane and n-octanol by a mixed aqueous solution of cationic-anionic surfactants, J. Colloid Interface Sci. 144 (1991) 185–190.

[10] L. Zhang, P. Li, X. Liu, L. Du, E. Wang, The effect of template phase on the structures of as-synthesized silica nanoparticles with fragile didodecyldimethylammonium bromide vesicles as templates, Adv. Mater. 19 (2007) 4279–4283.

[11] X.Z. Hu, H.N. Gong, Z.Y. Li, S. Ruane, H.Y. Liu, E. Pambou, C. Bawn, S. King, K. Ma, P.X. Li, What happens when pesticides are solubilized in nonionic surfactant micelles, J. Colloid Interface Sci. 541 (2019) 175–182.

[12] X.M. Ge, M.Y. Wei, S.N. He, W.E. Yuan, Advances of non-ionic surfactant vesicles (niosomes) and their application in drug delivery, Pharmaceutics 11 (2019) 55-55.

[13] R.C.G. Lopes, O.F. Silvestre, A.R. Faria, M.L.C. do Vale, E.F. Marques, J.B. Nieder, Surface charge tunable catanionic vesicles based on serine-derived surfactants as

[14] efficient nanocarriers for the delivery of the anticancer drug doxorubicin, Nanoscale 11 (2019) 5932–5941.

[14] Z. Li, H.R. Wu, Y. Hu, X. Chen, Y.J. Yuan, Y.L. Luo, J.R. Hou, B.J. Bai, W.L. Kang, Ultra-low interfacial tension biobased and catanionic surfactants for low permeability reservoirs, J. Mol. Liq. 309 (2020), 113099-113099.

[15] X. Han, X.H. Cheng, J. Wang, J.B. Huang, Application of anion-cation pair surfactant systems to achieve ultra-low oil-water interfacial tension, Acta Phys. -Chim. Sin. 28 (2012) 146–153.

[16] Z.J. Yu, G.X. Zhao, The physicochemical properties of aqueous mixtures of cationic-anionic surfactants: I. The effect of chain length symmetry, J. Colloid Interface Sci. 130 (1989) 414–420.

[17] F.M. Menger, J.S. Keiper, Gemini surfactants, Angew. Chem. Int. Ed. 39 (2000) 1906–1920.

[18] M.J. Qazi, S.J. Schlegel, E.H. Backus, M. Bonn, D. Bonn, N. Shahidzadeh, Dynamic surface tension of surfactants in the presence of high salt concentrations, Langmuir 36 (2020) 7956–7964.

[19] D.F. Yu, X. Huang, M.L. Deng, Y.Y. Lin, L.X. Jiang, J.B. Huang, Y.L. Wang, Effects of inorganic and organic salts on aggregation behavior of cationic gemini surfactants, J. Phys. Chem. B 114 (2010) 14955–14964.

[20] L. Chen, J.X. Xiao, K. Ruan, J.M. Ma, Homogeneous solutions of equimolar mixed cationic– anionic surfactants, Langmuir 18 (2002) 7250–7252.

[21] J. Eastoe, J. Dalton, P. Rogueda, D. Sharpe, J.F. Dong, J.R.P. Webster, Interfacial properties of a catanionic surfactant, Langmuir 12 (1996) 2706–2711.

[22] S. Rajkhowa, S. Mahiuddin, J. Dey, S. Kumar, V. Aswal, R. Biswas, J. Kohlbrecher, K. Ismail, The effect of temperature, composition and alcohols on the microstructures of catanionic mixtures of sodium dodecylsulfate and cetyltrimethylammonium bromide in water, Soft Matter 13 (2017) 3556–3567.

[23] E.W. Kaler, A.K. Murthy, B.E. Rodriguez, J.A.N. Zasadzinski, Spontaneous vesicle formation in aqueous mixtures of single-tailed surfactants, Science 245 (1989) 1371–1374.

[24] J.C. Hao, H. Hoffmann, Self-assembled structures in excess and salt-free catanionic surfactant solutions, Curr. Opin. Colloid Interface Sci. 9 (2004) 279–293.

[25] L.X. Jiang, K. Wang, M.L. Deng, Y.L. Wang, J.B. Huang, Bile salt-induced vesicle-to-micelle transition in catanionic surfactant systems: steric and electrostatic interactions, Langmuir 24 (2008) 4600–4606.

[26] X. Xiao, Y. Qiao, Z.R. Xu, T.Y. Wu, Y.X. Wu, Z. Ling, Y. Yan, J.B. Huang, Enzyme-Responsive Aqueous Two-Phase Systems in a Cationic–Anionic Surfactant Mixture, Langmuir 37 (2021) 13125–13131.

[27] H.Q. Yin, Y.Y. Lin, J.B. Huang, Microstructures and rheological dynamics of viscoelastic solutions in a catanionic surfactant system, J. Colloid Interface Sci. 338 (2009) 177–183.

[28] M. Yu, Z. Liu, Y. Du, C. Ma, Y. Yan, J. Huang, Endowing a light-inert aqueous surfactant two-phase system with photoresponsiveness by introducing a trojan horse, ACS Appl. Mater. Interfaces 11 (2019) 15103–15110.

[29] T. Bramer, N. Dew, K. Edsman, Pharmaceutical applications for catanionic mixtures, J. Pharm. Pharm. 59 (2007) 1319–1334.

[30] H. Jia, P. Lian, X. Leng, Y.G. Han, Q.X. Wang, K. Jia, X.P. Niu, M.Z. Guo, H. Yan, K. H. Lv, Mechanism studies on the application of the mixed cationic/anionic surfactant systems to enhance oil recovery, Fuel 258 (2019), 116156-116156.

[31] Y.C. Li, W.D. Zhang, B.L. Kong, M. Puerto, X.N. Bao, O. Sha, Z.Q. Shen, Y.Q. Yang, Y.H. Liu, S.Y. Gu, Mixtures of anionic/cationic surfactants: a new approach for enhanced oil recovery in low-salinity, high-temperature sandstone reservoir, SPE J. 21 (2016) 1164–1177.

[32] C. Wang, X.L. Cao, L.L. Guo, Z.C. Xu, L. Zhang, Q.T. Gong, L. Zhang, S. Zhao, Effect of molecular structure of catanionic surfactant mixtures on their interfacial properties, Colloids Surf. A Physicochem. Eng. Asp. 509 (2016) 601–612.

[33] L.X. Jiang, M.L. Deng, Y.L. Wang, D.H. Liang, Y. Yan, J.B. Huang, Special effect of β-cyclodextrin on the aggregation behavior of mixed cationic/anionic surfactant systems, J. Phys. Chem. B 113 (2009) 7498–7504.

[34] G.X. Zhao, J.X. Xiao, Surface activity of dodecyltrialkylammonium bromide and its mixture with sodium dodecylsulfate, Acta Phys. -Chim. Sin. 11 (1995) 785–790.

[35] J.X. Xiao, U. Sivars, F. Tjerneld, Phase behavior and protein partitioning in aqueous two-phase systems of cationic–anionic surfactant mixtures, J. Chromatogr. B 743 (2000) 327–338.

[36] H.Q. Yin, M. Mao, J.B. Huang, H.L. Fu, Two-phase region in the DTAB/SL mixed surfactant system, Langmuir 18 (2002) 9198–9203.

[37] G.X. Zhao, J.X. Xiao, Aqueous two-phase systems of the aqueous mixtures of cationic–anionic surfactants, J. Colloid Interface Sci. 177 (1996) 513–518.

[38] M. Mao, J.B. Huang, B.Y. Zhu, J.P. Ye, The transition from vesicles to micelles induced by octane in aqueous surfactant two-phase systems, J. Phys. Chem. B 106 (2002) 219–225.

[39] J.B. Huang, R. Yang, B.Y. Zhu, X. He, H.L. Fu, Vesicle formation of 1: 1 cationic and anionic surfactant mixtures in N, N-dimethylformamide and tetrahydrofuran solutions, Colloids Surf. A Physicochem. Eng. Asp. 174 (2000) 403–410.

[40] R.D. Falcone, N.M. Correa, J.J. Silber, Amphiphilic ionic liquids as sustainable components to formulate promising vesicles to be used in nanomedicine, Curr. Opin. Green. Sustain. Chem. 26 (2020), 100382-100382.

[41] C.C. Villa, N.M. Correa, J.J. Silber, F. Moyano, R.D. Falcone, Singularities in the physicochemical properties of spontaneous AOT-BHD unilamellar vesicles in comparison with DOPC vesicles, Phys. Chem. Chem. Phys. 17 (2015) 17112–17121.

[42] C.C. Villa, F. Moyano, M. Ceolin, J.J. Silber, R.D. Falcone, N.M. Correa, A unique ionic liquid with amphiphilic properties that can form reverse micelles and spontaneous unilamellar vesicles, Chem. Eur. J. 18 (2012) 15598–15601.